

2014

The scroll compressor with internal cooling system – conception and CFD analysis

Józef Rak

Wrocław University of Technology, Poland, jozef.rak@pwr.wroc.pl

Sławomir Pietrowicz

Wrocław University of Technology, Poland, slawomir.pietrowicz@pwr.wroc.pl

Zbigniew Gnutek

Wrocław University of Technology, Poland, zbigniew.gnutek@pwr.wroc.pl

Follow this and additional works at: <https://docs.lib.purdue.edu/icec>

Rak, Józef; Pietrowicz, Sławomir; and Gnutek, Zbigniew, "The scroll compressor with internal cooling system – conception and CFD analysis" (2014). *International Compressor Engineering Conference*. Paper 2364.
<https://docs.lib.purdue.edu/icec/2364>

This document has been made available through Purdue e-Pubs, a service of the Purdue University Libraries. Please contact epubs@purdue.edu for additional information.

Complete proceedings may be acquired in print and on CD-ROM directly from the Ray W. Herrick Laboratories at <https://engineering.purdue.edu/Herrick/Events/orderlit.html>

The scroll compressor with internal cooling system – conception and CFD analysis

Jozef RAK^{1*}, Slawomir PIETROWICZ², Zbigniew Gnutek³

¹Wroclaw University of Technology, Department of Thermodynamics,
Wroclaw, Poland
jozef.rak@pwr.edu.pl

²Wroclaw University of Technology, Department of Thermodynamics,
Wroclaw, Poland
slawomir.pietrowicz@pwr.edu.pl

³Wroclaw University of Technology, Department of Thermodynamics,
Wroclaw, Poland
zbigniew.gnutek@pwr.edu.pl

* Corresponding Author

ABSTRACT

In the paper a new kind of an oil – free scroll compressor is analyzed. To satisfy the working conditions and high operational reliability of the system a geometry of the moving and fixed scrolls was modified. In the central parts of the scroll elements the special chambers were created and used as a space for internal cooling of compressed medium. For analyzing the thermal – flow processes in the working chamber the finite volume method was used and carried out in ANSYS CFX software. This paper describes the system, the applied moving boundaries, the initial conditions and the influence of the modified vanes shape on the output parameters. The results obtained for modified geometry were compared with the “classical” geometry for the same initial conditions.

1. INTRODUCTION

The numerical CFD modeling of the scroll compressor chamber was introduced in order to compare the two concepts of scroll machines. The first one is the classical idea based on the involute scroll (Fig. 1a) and the second one is the modified shape of the vanes proposed in Bush, et al. (1994) and Pietrowicz (2003). The concept shown in the Figure 1b was to make a curve which is a combination of involute and a curve described in the plane of complex numbers. The novel design has shorter edge length what implies less material used, shorter machine tool work and also shortens a compression cycle for the same parameters. Furthermore a single working chamber has different shapes during the process, especially close to the discharge area where the long tail form can be noticed. Another distinctive feature is the relatively large space inside the vanes. It may be utilized to install a cooling system which potentially can improve the compression process by making it more isothermal and will be an object of further research separately.

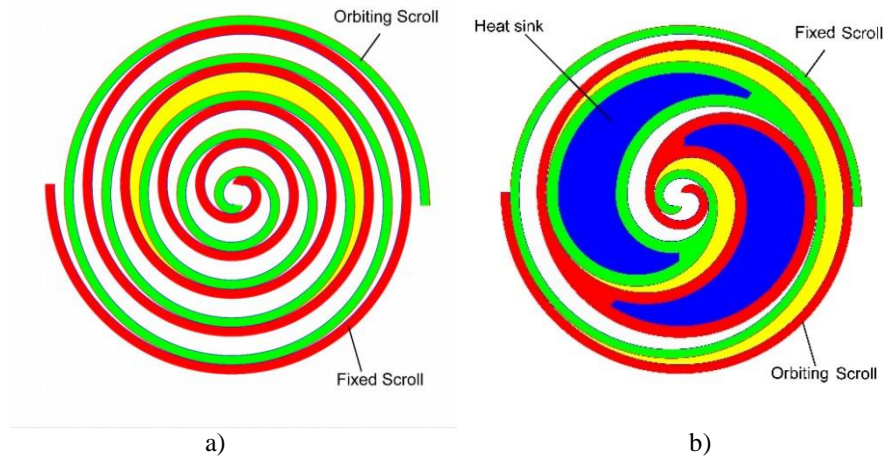


Figure 1: Scroll geometries comparison, a) classic, b) modified

Considering the differences in the geometry a CFD calculations of the single working chambers was performed with use of the user defined node displacement method. Two-dimensional simulation with the use of finite volume method was chosen. The emphasis was placed on dynamic and thermal properties.

2. GEOMETRIES

The scrolls are both designed for the same pressure ratio and mass flow rate. The first vane shape is a widely used involute represented, in Cartesian coordinates, by the Equation (1):

$$\begin{cases} x(\alpha) = r(\cos\alpha + a\sin\alpha) \pm \frac{g}{2}\sin\alpha \\ y(\alpha) = r(\sin\alpha - a\cos\alpha) \mp \frac{g}{2}\sin\alpha \end{cases} \quad (1)$$

with evolute angle $r=1.9$ mm and spiral thickness $g=3$ mm. Sequence is approximately 1.5 shaft revenue. The modified vane profile is based on a hybrid curve as in Equation (2) (Bush, et al 1994):

$$\vec{P} = R_s(\psi)e^{i\psi} + R_g(\psi)e^{i(\psi+\frac{\pi}{2})} \quad (2)$$

Sequence is less than one revenue what is a shorter and, in consequence, the number of simultaneously working chambers is smaller. Furthermore a greater compression work is performed in the discharge area. The geometries comparison is presented in Figure 2.

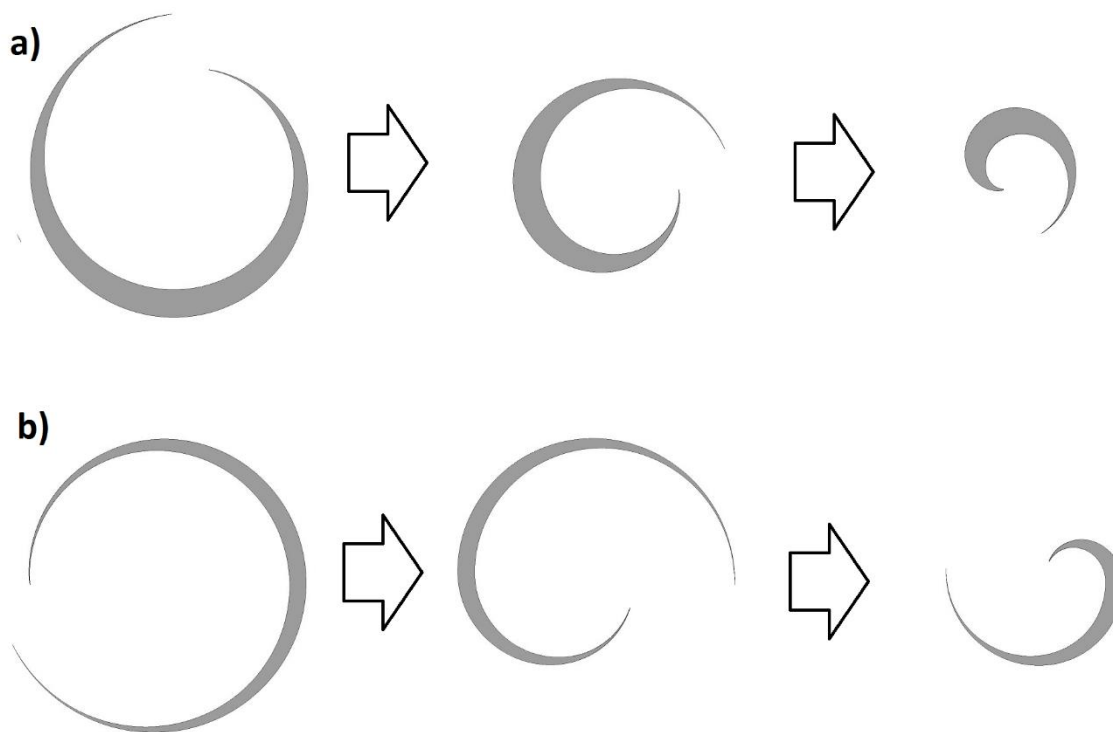


Figure 2: Compression chambers deformation, a) classic, b) modified

The single chamber deformation for each geometry is presented in the Figure 2. It may be noticed that the hybrid shape is longer and narrower comparing with the involute chamber. The mathematical formula describing this observation may be derived from the sinuosity of the walls. Sinuosity S , given in Equation (3) is defined as a length of a curve divided by a shortest distance between its ends. The difference between inner and outer wall sinuosities, shown in Equation (4), is a characteristic feature of a chamber and effects on the thermal-flow behavior of the medium.

$$S = \frac{L}{l} \quad (3)$$

$$S = \frac{L_{out} - L_{in}}{l} \quad (4)$$

The magnitudes of S parameter are presented in Figure 3.

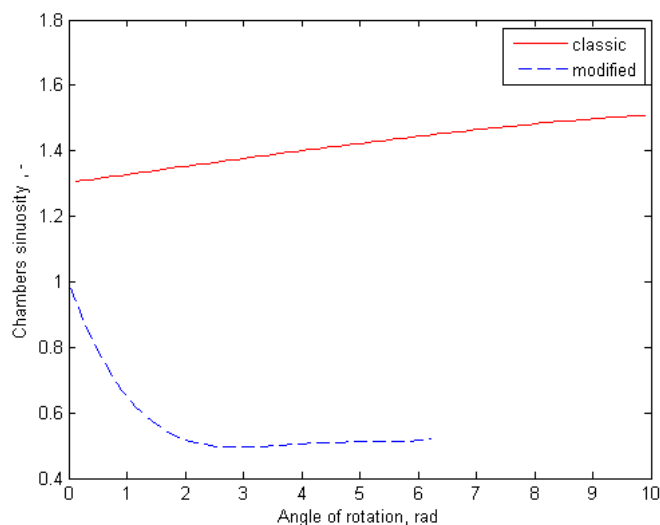


Figure 3: Chambers sinusities comparison

Both simulations concerns the process phase between suction and discharge, where the volume change is linear as presented in Figure 4. The initial nonlinearity in the modified geometry is a result of the transition from classical into new shape.

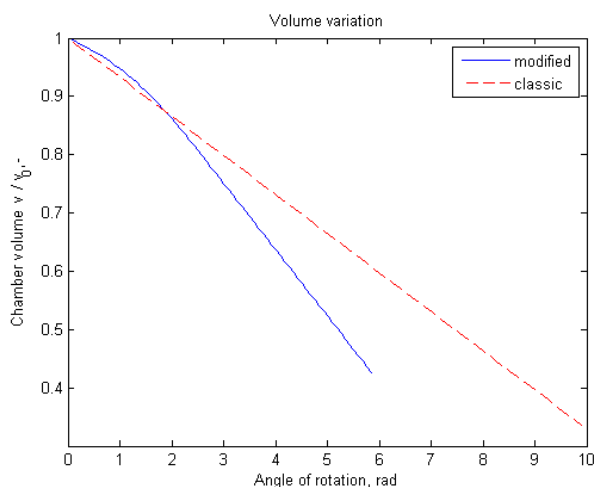


Figure 4: The rate of chamber volume change during the compression process

2. NUMERICAL MODEL

In order to perform the computations a series of hexahedral meshes were used. The each mesh was made from 624720 elements. The automatic meshing script was made in tcl language in order to generate the computational mesh every time step, based on a given geometry. It assured the consistency of the meshes topologies, preserved a quality and brought the data for user defined node displacement.

2.2 Equations, boundary and initial conditions

During the simulation the standard sort of equations were solved with the use of finite volume method and corrected for the moving/deforming boundary conditions. These were Navier-Stokes with a turbulence model and conjugate heat transfer. In order to compare the thermodynamic and fluid flow properties, the same simplified initial and boundary conditions (listed in Table 1) were applied.

Table 1: Model boundary conditions

Medium	air, ideal gas
Suction pressure	1 bar
Suction temperature	300 K
Walls	adiabatic
Turbulence model	k-epsilon
Wall function	scalable
Scroll rotational velocity	750 and 1500 rpm
Leakage	no leakage
Vanes deformation	no deformation

In order to estimate the wall heat transfer coefficient a similar method to Ooi (2004) was chosen. Since the flow was assumed to be turbulent with a scalable wall function, a following formula was used:

$$h = \frac{\rho c_p u^*}{T^+} \quad (5)$$

where:

$$u^* = C_\mu^{0.25} k^{0.5}$$

$$T^+ = 2.12 \ln y^* + \beta$$

$$\beta = \left(3.85 Pr^{\frac{1}{3}} - 1.3 \right)^2 + 2.12 \ln Pr$$

$$y^* = \frac{u^* \cdot \Delta n / 4}{\nu}$$

3. THE RESULTS

The average values of pressure and temperature over the chamber were calculated and compared to the curves determined by zero-dimension adiabatic compression:

$$p_2 = p_1 \left(\frac{v_1}{v_2} \right)^\gamma \quad (6)$$

$$T_2 = T_1 \left(\frac{v_1}{v_2} \right)^{\gamma-1} \quad (7)$$

Above equations are legitimate with the assumption that the process is free of leakage. The results are presented in the Figures 5 and 6 respectively. The error is rising with the transient calculation total time. The maximum errors are 2% for the pressure and 1% for the temperature.

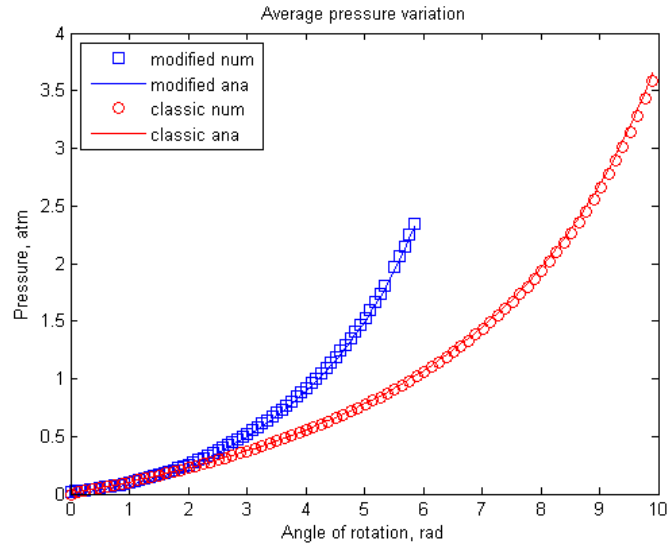


Figure 5: Average pressure over the chamber during the compression process

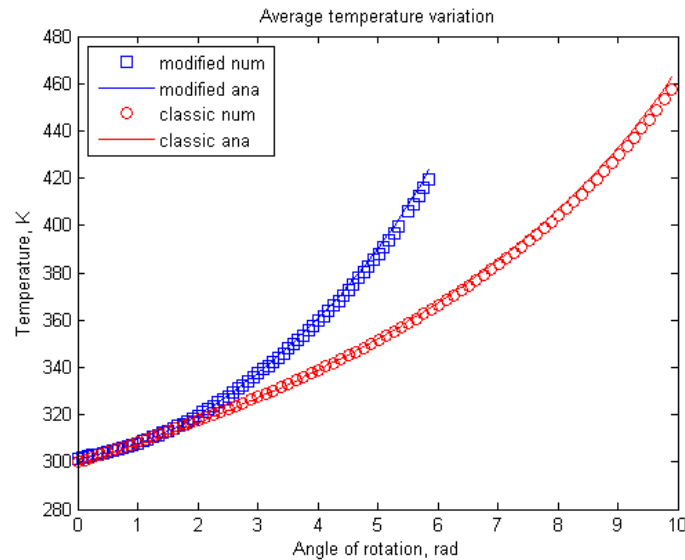


Figure 6: Average temperature over the chamber during the compression process

The wall heat transfer coefficient was calculated, using the formula (5), for two rotational speeds in each scroll design (Figure 7). In all of the cases the magnitude is rising logarithmically with the orbiting angle. The coefficient for the modified chamber is up to three times larger compared to the conventional solution. The rotational speed has an influence on the coefficient value especially in the beginning of the compression cycle (Fig. 8).

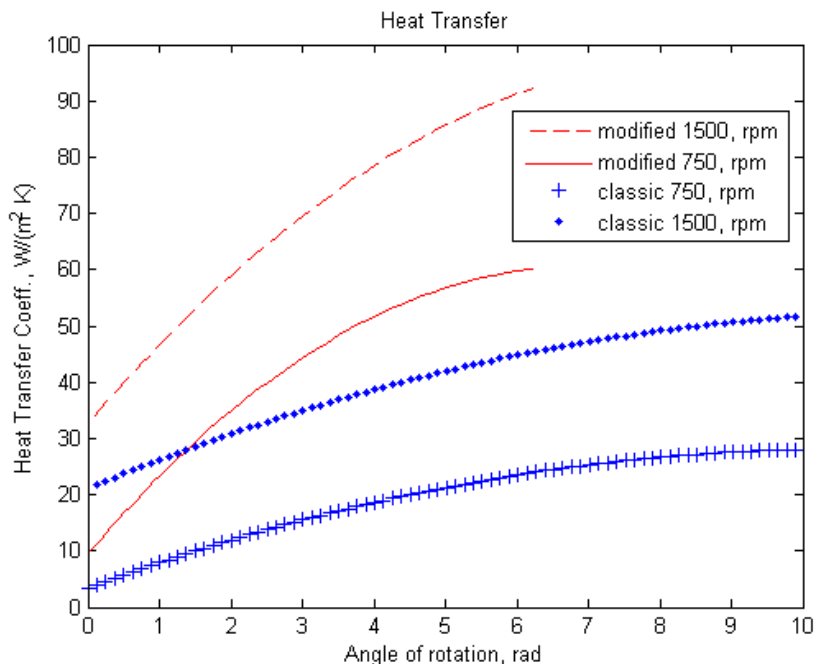


Figure 7: Average heat transfer coefficient over the outer chamber wall

The heat transfer coefficient ratio between 1500 rpm and 750 rpm is presented in Fig. 8. The rotational speed is more significant in the involute geometry. In both cases the ratio is converging to a constant value after about half of compression process.

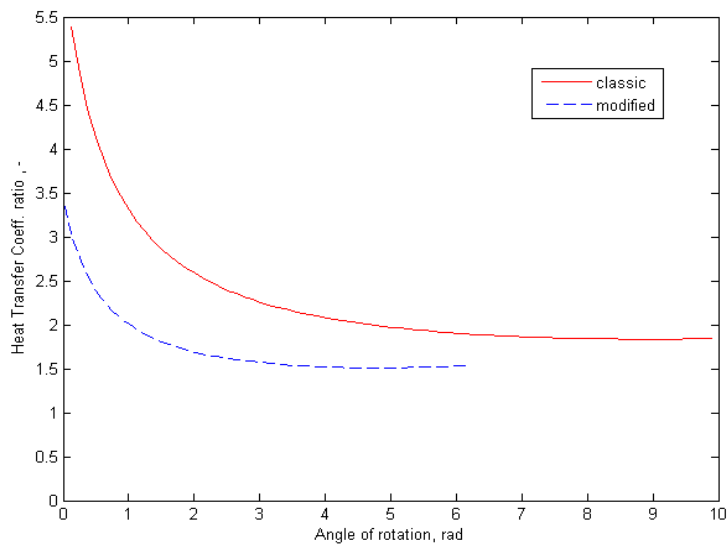


Figure 8: Heat transfer coeff. ratio $\frac{h_{1500\ rpm}}{h_{750\ rpm}}$

In the Figure 9 a pressure distribution in the working chamber is presented for. The pressure fields are evolving similarly for both scroll designs starting with circumferential and gradually progressing into more radial distribution.

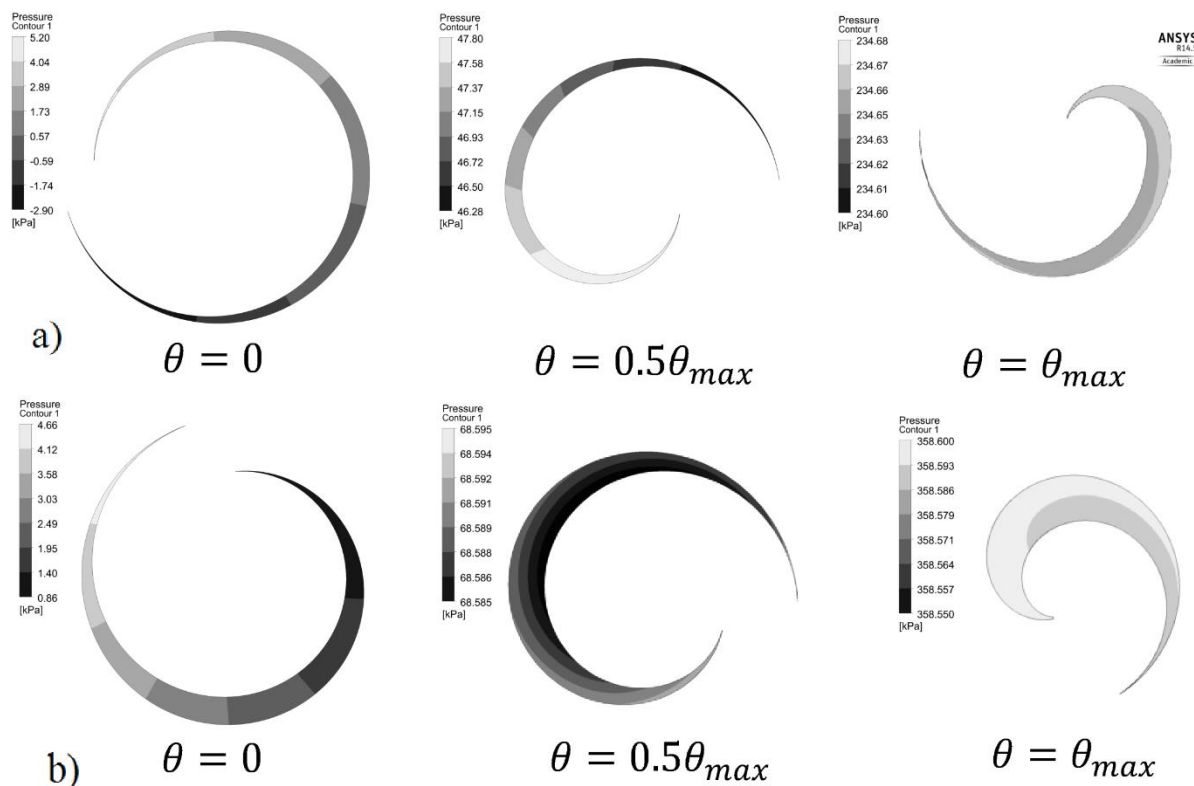


Figure 9: Pressure distribution over the working chamber a) hybrid, b) classic

3. SUMMARY

The concept of an oil-free scroll compressor with modified vanes shape was studied. A numerical simulation of an idealized non-leakage, adiabatic case was performed to compare it to a classical geometry. In both chamber geometries there is a very good agreement between numerical and analytical solutions. That benchmark confirms the validity of using the user defined node displacement method and its appliance for more complex modelling. Applying the same numerical procedure and boundary conditions assured that the only factor having an influence on the results is the chambers geometry. The hybrid vanes length is shorter and the sinusosity of a working chamber is lower than the conventional one. This means shorter compression cycle, lower vanes material usage and also different thermodynamic and flow behavior. The estimated wall heat transfer coefficient is larger in the new design compared to the classical one although it is less influenced by the rotational speed. Consequently there may be a better chance to increase the machines efficiency by making the compression process more isothermal.

NOMENCLATURE

c_p	heat capacity	(kJ/(kg K))
g	scroll vane thickness	(m)
h	heat transfer coefficient	(W/(m ² K))
L	chamber wall length	(m)
l	distance between common points	(m)
Δn	near wall grid spacing	(m)
P	vector	(-)
Pr	Prandtl number	(-)
r	evolute radius	(m)
R_g, R_s	vectors	(-)

S	sinuosity	(-)
T ⁺	non-dimensional temp.	(-)
α	involute angle	(rad)
γ	heat capacity ratio	(-)
θ	shaft angle	(rad)
ρ	density	(kg/m ³)
ψ	parameter	(-)

Subscript

in	chamber inner wall
out	chamber outer wall

REFERENCES

- Bush J. W., Beagle, W. P., Housman, M. E., 1994, Maximizing Scroll Compressor Displacement Using Generalized Wrap Geometry, *International Compressor Engineering Conference*, Purdue, p. 204-210.
- Ooi K.T., Zhu J., 2004, Convective heat transfer in a scroll compressor chamber: a 2-D simulation, *International Journal of Thermal Sciences*, vol. 43, no. 7, p. 677-688
- Pietrowicz S., 2003 The modelling of thermal – flow processes in scroll machines, Ph.D. Thesis, Wrocław University of Technology, Wrocław 2003 (in Polish). Wrocław University of Technology, Wrocław

ACKNOWLEDGEMENT

Calculations have been carried out using resources provided by Wrocław Centre for Networking and Supercomputing (<http://wcss.pl>), grant No. 278.